MASSLESS SCALAR FIELD COLLAPSE IN BRANS-DICKE THEORY

APPROVED:

_____

_____

MASSLESS SCALAR FIELD COLLAPSE IN BRANS-DICKE THEORY

by

Steven Lawrence Liebling, A.B.

THESIS

Presented to the Faculty of the Graduate School of

The University of Texas at Austin

in Partial Fulfillment

of the Requirements

for the Degree of

MASTER OF ARTS

THE UNIVERSITY OF TEXAS AT AUSTIN

May, 1995

I would like to dedicate this to all those who will be accidentally shot due to the legalization of concealed weapons in Texas.

Acknowledgments

I would like to thank Matthew Choptuik for his help and instruction. He has been very generous and patient while working with me at the console. I also thank him for the time he devoted towards making my routines adaptive by personally integrating them into his adaptive code.

I would also like to thank Lawrence C. Shepley, for his guidance and supervision.

The computations described in this thesis were performed using the resources of the High Performance Computing Facility and the Center for Relativity at The University of Texas at Austin. These computations were supported by the following grants: NSF PHY9310083 (Richard A. Matzner), NSF PHY9318152 (ARPA supplemented, Richard A. Matzner *et al*), and a Cray Research Grant (Richard A. Matzner).

Steven Lawrence Liebling

The University of Texas at Austin

May, 1995

MASSLESS SCALAR FIELD COLLAPSE IN BRANS-DICKE THEORY

Steven Lawrence Liebling, M.A.
The University of Texas at Austin, 1995

Supervisor: Lawrence C. Shepley

Using the adaptive mesh code of Matthew Choptuik, I have modeled a spherically symmetric, time-dependent spacetime in the Brans-Dicke theory with a minimally coupled scalar field as a source term. The constraint equations for initial data on a 3-dimensional slice of the spacetime are solved, and then evolved using the adaptive code. As with the scalar field collapse in general relativity, data which lead to black hole formation and those which do not are separated by some critical value of a parameter determining the strength of the initial pulse. Also, for those initial parameters serving to create a black hole upon collapse, the logarithm of the black hole mass is found to scale with the logarithm of the distance from a critical value of some parameter. Finally, for data near the critical value, discrete scaling in time and space of the waveform is observed. These critical phenomena are quite similar to those found by Choptuik. Results for both the mass scaling exponent, γ, and the scale periodic exponent, Δ_ρ, are in agreement with those found by Choptuik for the minimally coupled, scalar field in Einstein gravity.

Table of Contents

List of Figures

Chapter 1

Introduction

More than three-quarters of a century after Einstein first formulated his General Theory of Relativity, researchers are still examining its implications. The non-linearity of the Einstein field equations and the difficulty in finding their solutions have spawned the growth of numerical relativity. Ever-increasing computer power has nurtured this growth.

As complex as the solutions are, and as expensive as the ultimate in computer power is, simple problems in general relativity merit research. Spherically symmetric universes provide the simplest of non-trivial solutions involving only one spatial coordinate and a time coordinate. Work by Choptuik [Choptuik,1993] has already investigated the behavior of a scalar field in a spherically symmetric general relativistic universe.

In his work, Choptuik discovered critical behavior and scale periodicity of solutions forming black holes. Specifically he found, given some initial waveform for the scalar field parameterized by some parameter p (e.g. Gaussian amplitude or width), a specific value for p could be found, p^*, such that fields with $p > p^*$ formed a black hole while those with $p < p^*$ did not. Further, with the critical solution $p = p^*$ of any initial waveform (e.g. Gaussian, tanh, etc.), its evolution approached a universally identical spacetime. He also found for data with $p > p^*$, the logarithm of the black hole mass scaled with the

logarithm of $p - p^*$. Specifically, $M_{BH} \propto (p - p^*)^\gamma$ with $\gamma \approx 0.37$.

This thesis seeks to look again at the massless scalar field, but this time in a universe ruled by Brans-Dicke Theory instead of general relativity. Work presented here seeks similar effects when the gravitational constant is allowed to vary. The work is motivated both by a desire to study Brans-Dicke theory and also as an introduction to numerical relativity with a very tractable problem in numerical modeling.

1.1 Reasons to study Brans-Dicke Theory

Brans-Dicke theory differentiates itself from general relativity by allowing the gravitational constant G to vary[Brans,1961]. This freedom is motivated by the idea that inertial mass should be defined with respect to the rest of the mass of the universe. Experimenters researching whether the observed Universe follows general relativity have succeeded only in limiting any variance of G to extremely small values. As such, Brans-Dicke theory is not considered to represent reality.

Brans-Dicke theory does present a different environment within which one can look for interesting critical phenomena. Particularly of interest is the theory's allowance of gravitational radiation in a spherically symmetric universe. In general relativity, gravitational radiation lacks any monopole or dipole sources and thus does not appear in spherically symmetric universes. However, Brans-Dicke universes, with the freedom in its scalar field, allow for such radiation. Scheel mentions the possibility that gravitational wave detectors such as LIGO may be able to differentiate between general relativity

and Brans-Dicke radiation[Scheel,1995b].

Though experiments have shown any possible variance in G to be negligible, theorists seeking a method for inflation discuss the possibility that at early times in the Big Bang, the effects might have been significant. These theorists have yet to fully resolve the reasons for the homogeneity of the Universe. Inflation appears to be a possible unifying theory, and the simplest methods for inflation would involve a scalar/tensor theory of gravity such as Brans-Dicke [Scheel,1995b].

1.2 Other Related Research

Other research in Brans-Dicke theory has been minimal lately. Scheel, Shapiro, and Teukolsky model collisionless matter in a Brans-Dicke universe by initially avoiding the singularity, and then truncating their grid inside the apparent horizon [Scheel,1995a]. In the second part of their paper, they describe the results obtained with the numerical code, showing that the final black holes produced are equivalent to those of Einstein's theory [Scheel,1995b].

Choptuik's work [Choptuik,1993] has elicited many responses both to duplicate and to explain the effects he observed. David Garfinkle has produced similar results [Garfinkle,1995]. A group in Japan has recently applied renormalization group theory to the similar problem of a radiation fluid collapse and found a value for the critical exponent of $\gamma \simeq 0.356$ [Koike,1995].

1.3 Expected Implications

The possibility of observing interesting phenomena similar to those of Choptuik [Choptuik,1993] motivates this research. Of course interesting results different than those found for general relativity would likewise be satisfactory. Further, the research has served as a worthwhile introduction to numerical relativity.

The research discussed here studies the evolution of a minimally coupled, massless, Klein-Gordon scalar field within the framework of a universe ruled by the Brans-Dicke field equations [Brans,1961]. In Chapter 2, I derive the governing equations from the Brans-Dicke theory. The conclusion of Chapter 2 discusses the process by which I have solved these equations computationally. Namely, I briefly discuss how the highly non-linear, differential equations are approximated by finite differencing whereby differentials appearing in the equations are replaced by finite differences.

Chapter 3 discusses the results. Specifically, I present both the mass scaling and the scale periodic behavior which had been anticipated. Finally, conclusions are presented in Chapter 4.

Chapter 2

Methodology

The field equations of general relativity provide equations with which to determine the geometry of the universe at all times and space. In keeping with dynamics as conventionally studied in physics, these four-dimensional equations are re-written to follow data on a three-dimensional slice in time. I take an initial slice, $\Sigma_{t=t_o}$, and determine the evolution equations to construct the four-dimensional universe. Some of the field equations then necessarily constrain the geometry of this slice. This method is called the 3+1 formalism and was first developed by Arnowitt, Deser and Misner[ADM,1962]. Work here has relied primarily on the discussions found in [Misner,1973] and [York,1979].

For simplicity, I adopt the convention of letting the speed of light be unity such that $c = 1$. Further, as the Einstein frame contains the universal gravitational constant, G, I let $G = 1$. In addition, Greek letters span the four dimensions running $0 \ldots 3$, while Latin indices span the spatial indices $1 \ldots 3$.

2.1 3+1 Overview

2.1.1 Slicing, lapse and shift

In constructing the four-dimensional universe, one begins by taking an initial, three-dimensional, spacelike hypersurface, $\Sigma_{t=t_o}$ and evolves it to other slices, Σ_t. Upon each of these slices, a metric is defined, which is called

the three-metric, ${}^{(3)}g_{ij}$. This metric yields the proper distances between points on that surface. The evolution of this three-metric to other slices is dependent on the choice of slicing.

With the universe sliced into this one parameter family of slices, their relation to each other must be formally expressed to preserve the original structure of the four-dimensional space. For an observer deciding to travel between slices, she is constrained by the arrangement of the slices. In other words, the observer's proper time and position must be connected from slice to slice. Defining a function of both space and time which measures the proper time between slices constrains the last degree of freedom of the three-dimensional slice. With this function, termed the *lapse*, and a three-vector describing how coordinate points shift between the slices, the four-dimensional metric can be constructed from the the three-metric.

Letting $\alpha(x^i, t)$ be a measure of the proper time difference between two slices measured by an observer moving orthogonally to the slices, and $\beta^i(x^i, t)$ be a measure of the infinitesimal shift of the spatial coordinates relative to normal propagation, then the general four-metric, ${}^{(4)}g_{\mu\nu}$, can be written

$$ds^2 = {}^{(3)}g_{ij}(dx^i + \beta^i dt)(dx^j + \beta^j dt) - (\alpha dt)^2 \tag{2.1}$$

Given this metric, one can compute the Einstein tensor, $G_{\mu\nu}$, which describes the geometry of the spacetime. Using Einstein's field equations

$$G_{\mu\nu} = R_{\mu\nu} - \frac{1}{2}g_{\mu\nu}R = 8\pi T_{\mu\nu} \tag{2.2}$$

where $R_{\mu\nu}$ is the Ricci curvature tensor, R, the Ricci scalar, is the trace of

the curvature tensor, $R \equiv g^{\mu\nu}R_{\mu\nu}$, and $T_{\mu\nu}$ is the stress-energy tensor, one can obtain the evolution and constraint equations for general relativity.

Einstein's field equations consist of ten independent equations, which, in the 3+1 formalism, decompose into six evolution equations and four constraint equations. The constraint equations are obtained by re-expressing the Einstein tensor in terms of a three-tensor, K_{ij}, and the three-geometry curvature scalar, ${}^{(3)}R$. The three tensor K_{ij} is termed the *extrinsic curvature* and represents the curvature of a slice with respect to the enveloping four-space.

Each three-dimensional slice resides in a four-dimensional manifold. A normal, n^{μ}, defined at all points on that slice represents the orientation of that slice with respect to the four-geometry just as a normal to a plane in Euclidean three-space identifies the orientation of the plane in that space. Clearly, were this normal to remain everywhere constant on the slice, the slice would have no extrinsic curvature. Hence, it is in terms of changes in the normal with respect to differing position on the slice that extrinsic curvature is defined. Mathematically, this idea is expressed as [Misner,1973]

$$ {}^{(4)}\nabla_i n_j = -K_{ij} \tag{2.3} $$

This formulation allows certain components of the left side of equation (2.2) to be rewritten in terms of quantities which are defined on a single slice [Misner,1973]

$$ -G^0_0 = \frac{1}{2}{}^{(3)}R + \frac{1}{2}K^2 - \frac{1}{2}K^m{}_j K^j{}_m = 8\pi\rho \tag{2.4} $$

$$ -G^n_i = K^m_{i|m} - K_{,i} = 8\pi j_i \tag{2.5} $$

where K is the trace of the extrinsic curvature, $K \equiv g^{ij}K_{ij} \equiv g_{ij}K^{ij} = K^i_i$. The symbol "|" represents covariant differentiation in the three-geometry. Here, ρ is the energy density and j_i is the momentum density defined as

$$\rho = n_\mu n_\nu T^{\mu\nu} \tag{2.6}$$

$$j_i = {}^{(3)}g_{ik}j^k = -n_\mu T^\mu_i \tag{2.7}$$

In addition, the spatial stress tensor S_{ij} is defined by $S_{ij} \equiv T_{ij}$.

By restricting the modeled universe to be spherically symmetric, the above expressions become simplified. The general three-metric, itself necessarily spherically symmetric, can be expressed in terms of two arbitrary functions of r and t, $a(r,t)$ and $b(r,t)$ [Choptuik,1986]. Working in spherical coordinates (t, r, ϕ, φ) yields

$${}^{(3)}g_{ij} = \begin{pmatrix} a^2 & 0 & 0 \\ 0 & b^2r^2 & 0 \\ 0 & 0 & b^2r^2\sin^2\theta \end{pmatrix} \tag{2.8}$$

so the four-metric becomes according to equation (2.1)

$${}^{(4)}g_{ij} = \begin{pmatrix} a^2\beta^2 - \alpha^2 & a^2\beta & 0 & 0 \\ a^2\beta & a^2 & 0 & 0 \\ 0 & 0 & b^2r^2 & 0 \\ 0 & 0 & 0 & b^2r^2\sin^2\theta \end{pmatrix} \tag{2.9}$$

Because of spherical symmetry, the shift vector has only one non-zero component $\beta^i = (\beta, 0, 0)$ with $\beta_i = {}^{(3)}g_{ij}\beta^j$. Spherical symmetry also implies that the extrinsic curvature is diagonal [Choptuik,1986].

$$K^i_j = \begin{pmatrix} K^r_r & 0 & 0 \\ 0 & K^\theta_\theta & 0 \\ 0 & 0 & K^\theta_\theta \end{pmatrix} \tag{2.10}$$

with both angular components equal by symmetry.

The equations (2.4, 2.5) in spherical symmetry have previously been solved by Choptuik [Choptuik,1986]. The Hamiltonian constraint (2.4) along with (2.6) takes the form

$$-\frac{2}{arb}\left(\left(\frac{(rb)'}{a}\right)' + \frac{1}{rb}\left(\left(\frac{rb}{a}(rb)'\right)' - a\right)\right) + 4K_r^r K_\theta^\theta + 2K_\theta^{\theta 2} = 16\pi\rho \quad (2.11)$$

while the momentum constraint (2.7) produces only one non-trivial equation

$$K_\theta^{\theta\prime} + \frac{(rb)'}{rb}\left(K_\theta^\theta - K_r^r\right) = 4\pi j_r \quad (2.12)$$

In addition, six evolution equations are derivable from (2.3) found in [Choptuik,1986] as

$$\dot{g}_{ij} = -2\alpha g_{ik}K_j^k + \beta^k g_{ij,k} + g_{ik}\beta_{,j}^k + g_{kj}\beta_{,i}^k \quad (2.13)$$

The Einstein equations which contain second derivatives of the metric components result in [Choptuik,1986]

$$\dot{K}_i^j = \beta^k K_{i,k}^j + K_k^j \beta_{,i}^k - K_i^k \beta_{,k}^j - \alpha\big|_i^j + \alpha\left(R_i^j + KK_i^j + 4\pi\left(S-\rho\right)\delta_i^j - 8\pi S_i^j\right) \quad (2.14)$$

2.1.2 Polar/radial scheme

The above equations are tensor equations, and thus allow freedom in choosing the coordinate scheme. This freedom can be used to simplify further the equations. In accordance with the polar/radial scheme, I let $b = 1$ and $\dot{b} = 0$, so that the coordinate r is related to the proper surface area of a sphere with constant t and r, by $4\pi r^2$. In other words, integration of the metric over the area of a sphere yields a surface area of $4\pi r^2$.

With freedom in the choice of slicing, I choose a polar slicing scheme in which slices are chosen such that

$$\mathrm{Tr}K = K^i_i = K^r_r \tag{2.15}$$

This requirement immediately implies that

$$K^\theta_\theta = 0 = K^\phi_\phi \tag{2.16}$$

One nicety of the polar/radial scheme is that the evolution equation for the metric function b obtained from (2.13)

$$\dot{b} = -\alpha b K^\theta_\theta + \frac{\beta}{r}(rb)' \tag{2.17}$$

becomes, with $K^\theta_\theta = 0$ and $\dot{b} = 0$,

$$\beta = 0 \tag{2.18}$$

These gauge choices greatly simplify the equations in Section 2.1.1 so that the Hamiltonian constraint and slicing equation reduce to [Choptuik,1986]

$$\begin{aligned} -\frac{2}{a}\left(\left(\frac{1}{a}\right)' + \frac{1}{r}\left(\left(\frac{r}{a}\right)' - a\right)\right) &= 16\pi\rho \\ \alpha' + \left(\frac{1-a^2}{r} - \frac{a'}{a}\right)\alpha &= 0 \end{aligned} \tag{2.19}$$

2.2 Brans-Dicke Equations

Brans-Dicke theory asserts that inertia should be tied to the mass distribution of the Universe [Brans,1961] [Weinberg,1972]. This assertion led Brans and Dicke to the idea that the gravitational constant G should be dependent upon a scalar field ϕ which reflects the distribution of mass in the universe.

Brans and Dicke proposed, instead of using a constant gravitational constant G in the field equations, letting G vary over space and time. They defined G as the inverse of a scalar field ϕ such that $G = \phi^{-1}$. This addition of a scalar field necessitates an added term to the stress-energy tensor

$$G^{\mu\nu} = R^{\mu\nu} - \frac{1}{2} g^{\mu\nu} R = \frac{8\pi}{\phi} \left[T_M^{\mu\nu} + T_\phi^{\mu\nu} \right] \tag{2.20}$$

where $T_M^{\mu\nu}$ is the stress-energy tensor due to the matter and $T_\phi^{\mu\nu}$ is the contribution due to the Brans-Dicke field, ϕ.

They also proposed the simplest generally covariant field equation for the scalar field as

$$\Box\phi = 4\pi\lambda T_M \tag{2.21}$$

where T_M is the trace of the stress-energy tensor for matter $T_M = T_{M\mu}^{\mu}$. Here, λ is a constant representing the strength of the coupling of the Brans-Dicke field to matter. Also, for some arbitrary scalar field θ,

$$\Box\theta = \theta_{;\mu}{}^{;\mu} = \frac{1}{\Gamma} \left(\Gamma^{(4)} g^{\mu\nu} \theta_{,\mu} \right)_{,\nu} \tag{2.22}$$

where $\Gamma \equiv \sqrt{-{}^{(4)}g}$ and ";" represents covariant differentiation in the four-geometry. Through use of the Bianchi identities, Weinberg [Weinberg,1972] determines that the above equation yields

$$T_{\mu\nu}^{\phi} = \frac{\omega}{8\pi\phi} \left(\phi_{,\mu}\phi_{,\nu} - \frac{1}{2} g_{\mu\nu} \phi_{,\rho}\phi^{,\rho} \right) + \frac{1}{8\pi} \left(\phi_{,\mu,\nu} - g_{\mu\nu}\Box\phi \right) \tag{2.23}$$

with $\lambda = 2/(3 + 2\omega)$.

From inspection of equation (2.20), it appears that the Brans-Dicke equations can be found from the appropriate general relativity equations with

the transformations

$$\begin{aligned} \rho &\rightarrow \rho^{\phi} + \rho^{M} \\ j^{a} &\rightarrow j^{a}_{\phi} + j^{a}_{M} \\ S_{ab} &\rightarrow S^{\phi}_{ab} + S^{M}_{ab} \\ \kappa &\rightarrow \frac{\kappa}{\phi} \end{aligned} \tag{2.24}$$

where S_{ab} is the spatial-momentum tensor, and κ is simply a constant dependent on the system of units used. In the units used here, $\kappa = 8\pi$.

2.2.1 Transformation to Einstein Frame

The equations found for Brans-Dicke are quite similar to those of general relativity except for the appearance of an additional field ϕ. However, the equations can be transformed so that they more clearly coincide with those of general relativity. The model is then said to be in the Einstein frame. By such a transformation, the model will consist simply of two scalar fields, generically denoted as θ, obeying some general source equation dependent on the geometry

$$\Box\theta = S_{\theta} \tag{2.25}$$

where S_{θ} represents a general source term.

By transforming the metric as $g_{\mu\nu} \rightarrow f(x^{\mu})^{p} g_{\mu\nu}$ for some general scalar field f raised to some power p and some general metric, a change is introduced which effects a local change in scale. The transformation is said to be conformal because the transformation retains original angles between vectors [Wald,1984]. In particular, the physical metric representing the geometry in

the Brans-Dicke frame can be conformally transformed to the Einstein frame by using the Brans-Dicke field itself as the conformal factor

$$\begin{aligned} \bar{g}_{\mu\nu} &= \phi g_{\mu\nu} \\ \bar{g}^{\mu\nu} &= \phi^{-1} g^{\mu\nu} \\ \xi &\equiv \ln \phi \end{aligned} \tag{2.26}$$

where a bar over a variable indicates the variable defined in the Einstein frame. The actual physics of the problem occur in the Brans-Dicke frame which makes physical interpretations more difficult in the Einstein frame. This problem is deferred until Section 3.3. However, the transformation to the Einstein frame avoids the appearance of second derivatives of the Brans-Dicke field in the equations and thus greatly simplifies the equations.

In order to compute the equations of motion in the Einstein frame, the tensors $\bar{R}_{\mu\nu}$ and $\bar{R}$ must first be computed.

With the Christoffel symbols $\Gamma^{\mu}_{\nu\rho}$ defined as

$$\Gamma^{\mu}_{\nu\rho} = \frac{1}{2} g^{\mu\gamma} \left(g_{\gamma\nu,\rho} + g_{\gamma\rho,\nu} - g_{\nu\rho,\gamma} \right) \tag{2.27}$$

the transformed connections are [York,1979]

$$\begin{aligned} \bar{\Gamma}^{\alpha}_{\beta\gamma} &\equiv \frac{1}{2} \bar{g}^{\alpha\delta} \left(\bar{g}_{\delta\beta,\gamma} + \bar{g}_{\delta\gamma,\beta} - \bar{g}_{\beta\gamma,\delta} \right) \\ &= \Gamma^{\alpha}_{\beta\gamma} + \frac{1}{2} g^{\alpha\delta} \left(\xi_{,\gamma} g_{\delta\beta} + \xi_{,\beta} g_{\delta\gamma} - \xi_{,\delta} g_{\beta\gamma} \right) \\ &= \Gamma^{\alpha}_{\beta\gamma} + \delta^{\alpha}_{(\beta} \xi_{,\gamma)} - \frac{1}{2} g^{\alpha\sigma} g_{\beta\gamma} \xi_{,\sigma} \end{aligned} \tag{2.28}$$

where the parenthesis indicate symmetrization defined on a general tensor $W_{\beta\gamma}$ as

$$W_{(\beta\gamma)} = \frac{1}{2} \left(W_{\beta\gamma} + W_{\gamma\beta} \right) \tag{2.29}$$

and where δ^{α}_{β} is the Kronecker delta defined by

$$\delta^{\alpha}_{\beta} = \begin{cases} 1 & \text{if } \alpha = \beta \\ 0 & \text{otherwise} \end{cases} \tag{2.30}$$

With the Christoffel symbols in the Einstein frame computed, $\bar{R}_{\mu\nu}$ may be found by taking the general form in terms of some constants a, b, c, and d

$$\bar{R}_{\mu\nu} = R_{\mu\nu} + a\xi_{,\mu}\xi_{,\nu} + bg_{\mu\nu}\xi_{,\sigma}\xi^{,\sigma} + c\xi_{;\mu;\nu} + dg_{\mu\nu}\Box\xi \tag{2.31}$$

The necessary calculations are done in Wald [Wald,1984] with the result for $n = 4$ dimensions:

$$\bar{R}_{\mu\nu} = R_{\mu\nu} + \frac{1}{2}\xi_{,\mu}\xi_{,\nu} - \frac{1}{2}g_{\mu\nu}\xi_{,\sigma}\xi^{,\sigma} - \xi_{;\mu;\nu} - \frac{1}{2}g_{\mu\nu}\Box\xi \tag{2.32}$$

And with $\bar{R} = \bar{g}_{\mu\nu}\bar{R}_{\mu\nu} = \phi^{-1}g^{\mu\nu}\bar{R}_{\mu\nu}$,

$$\bar{R} = \phi^{-1}\left(R - \frac{3}{2}\xi_{,\sigma}\xi^{,\sigma} - 3\Box\xi\right) \tag{2.33}$$

At this point, the Einstein tensor components in the Einstein frame are found using the results (2.33) and (2.32):

$$\begin{aligned}
&\bar{R}_{\mu\nu} - \frac{1}{2}\bar{g}_{\mu\nu}\bar{R} \\
&= R_{\mu\nu} + \frac{1}{2}\xi_{,\mu}\xi_{,\nu} - \frac{1}{2}g_{\mu\nu}\xi_{,\sigma}\xi^{,\sigma} - \xi_{;\mu;\nu} - \frac{1}{2}g_{\mu\nu}\Box\xi - \frac{1}{2}g_{\mu\nu}R \\
&\quad - \frac{3}{4}g_{\mu\nu}\xi_{,\sigma}\xi^{,\sigma} + \frac{3}{2}g_{\mu\nu}\Box\xi \\
&= R_{\mu\nu} - \frac{1}{2}g_{\mu\nu}R + \frac{1}{2}\xi_{,\mu}\xi_{,\nu} + \frac{1}{4}g_{\mu\nu}\xi_{,\sigma}\xi^{,\sigma} - \xi_{;\mu;\nu} + g_{\mu\nu}\Box\xi \\
&= R_{\mu\nu} - \frac{1}{2}g_{\mu\nu}R + \frac{3}{2}\phi^{-2}\left(\phi_{,\mu}\phi_{,\nu} - \frac{1}{2}g_{\mu\nu}\phi_{,\sigma}\phi^{,\sigma}\right) - \\
&\quad \frac{1}{\phi}\left(\phi_{,\mu,\nu} - g_{\mu\nu}\Box\phi\right)
\end{aligned} \tag{2.34}$$

The original Brans-Dicke equation (2.20),

$$R_{\mu\nu} - \frac{1}{2} g_{\mu\nu} R = \frac{8\pi}{\phi} \left(T^{\phi}_{\mu\nu} + T^{M}_{\mu\nu} \right) \tag{2.35}$$

where $T^{\phi}_{\mu\nu}$ is given by equation (2.23), becomes using the previous results (2.34)

$$\begin{aligned} \bar{R}_{\mu\nu} - \frac{1}{2} \bar{g}_{\mu\nu} \bar{R} &= \\ -\frac{3}{2} \phi^{-2} \left(\phi_{,\mu} \phi_{,\nu} - \frac{1}{2} g_{\mu\nu} \phi_{,\sigma} \phi^{,\sigma} \right) &- \frac{\omega}{8\pi\phi} \left(\phi_{,\mu} \phi_{,\nu} - \frac{1}{2} g_{\mu\nu} \phi_{;\rho} \phi^{;\rho} \right) \\ &= \frac{8\pi}{\phi} T^{M}_{\mu\nu} \end{aligned} \tag{2.36}$$

Letting $\bar{T}_{\mu\nu} \equiv \phi^{-1} T_{\mu\nu}$ and once again using $\xi \equiv \ln \phi$ this becomes

$$\bar{G}_{\mu\nu} = \left(\frac{3 + 2\omega}{2} \right) \left(\xi_{,\mu} \xi_{,\nu} - \frac{1}{2} \bar{g}_{\mu\nu} \bar{g}^{\rho\sigma} \xi_{,\rho} \xi_{,\sigma} \right) + 8\pi \bar{T}^{M}_{\mu\nu} \tag{2.37}$$

From result (2.37) the equations of motion are ultimately derived (see Section 2.2.3).

With the scalar field satisfying the equation (2.21), the equation of motion of $\xi \equiv \ln \phi$ can be found

$$\begin{aligned} \Box \phi &= 4\pi \lambda T_M = g^{\mu\nu} (\phi_{,\mu})_{;\nu} \\ &= \phi \bar{g}_{\mu\nu} (\phi_{,\mu\nu} - (\bar{\Gamma}^{\gamma}_{\mu\nu} - \delta^{\gamma}_{(\mu} \xi_{\nu)} + \frac{1}{2} \bar{g}^{\gamma\rho} \bar{g}_{\mu\nu} \xi_{,\rho}) \phi_{,\gamma}) \\ &= \phi^2 \left(\phi^{-1} \bar{\Box} \phi - \phi^{-2} \bar{g}^{\mu\nu} \phi_{,\mu} \phi_{,\nu} \right) \\ &= \phi \bar{\Box} \phi - \bar{g}^{\mu\nu} \phi_{,\mu} \phi_{,\nu} \\ \Box \phi &= \phi^2 \bar{\Box} \xi \end{aligned} \tag{2.38}$$

Since $T = g^{\mu\nu} T_{\mu\nu} = (\phi \bar{g}^{\mu\nu})(\phi \bar{T}_{\mu\nu}) = \phi^2 \bar{T}$, this becomes

$$\bar{\Box} \xi = 4\pi \lambda \bar{T}_M \tag{2.39}$$

At this point, I introduce ψ to represent the massless, minimally coupled, Klein-Gordon scalar field. This field is a physical source to which the Brans-Dicke field can couple. To compute $\bar{T}_M$, the trace of the matter stress-energy, first the actual tensor $\bar{T}^M_{\mu\nu}$ in the Einstein frame is obtained from the original tensor $T^M_{\mu\nu}$

$$T^M_{\mu\nu} = \left(\psi_{,\mu}\psi_{,\nu} - \frac{1}{2}g_{\mu\nu}g^{\gamma\rho}\psi_{,\gamma}\psi_{,\rho}\right) \tag{2.40}$$

so that

$$\begin{aligned} \bar{T}^M_{\mu\nu} &= \frac{1}{\phi}T^M_{\mu\nu} \\ &= \frac{1}{\phi}\left(\psi_{,\mu}\psi_{,\nu} - \frac{1}{2}g_{\mu\nu}g^{\gamma\rho}\psi_{,\gamma}\psi_{,\rho}\right) \end{aligned} \tag{2.41}$$

From this, the trace is computed by contracting with the metric

$$\begin{aligned} \bar{T}_M &\equiv \bar{g}^{\mu\nu}\bar{T}^M_{\mu\nu} \\ &= \bar{g}^{\mu\nu}\left[\phi^{-1}\left(\psi_{,\mu}\psi_{,\nu} - \frac{1}{2}\bar{g}_{\mu\nu}\bar{g}^{\gamma\rho}\psi_{,\gamma}\psi_{,\rho}\right)\right] \\ &= \phi^{-1}\left(\psi^{,\nu}\psi_{,\nu} - \frac{1}{2}\left(\bar{g}^{\mu\nu}\bar{g}_{\mu\nu}\right)\psi^{,\rho}\psi_{,\rho}\right) \\ &= -\frac{1}{\phi}\psi^{,\nu}\psi_{,\nu} \end{aligned} \tag{2.42}$$

Equation (2.39), with the value for $\bar{T}_M$ found above, yields the equation of motion for ξ

$$\bar{\Box}\xi = -4\pi\lambda e^{-\xi}\psi^{,\nu}\psi_{,\nu} \tag{2.43}$$

With $\bar{G}_{\mu\nu}$ calculated using equation (2.37) and the other results, consistency can be checked via the contracted Bianchi identity in the Einstein frame [Choptuik,1995].

$$\bar{G}_{\mu\nu;}{}^{\nu} = \lambda^{-1}\left((\xi_{,\mu}\xi_{,\nu})^{;\nu} - \frac{1}{2}\bar{g}_{\mu\nu}\left(\xi_{,\rho}\xi^{,\rho}\right)^{;\nu}\right) + 8\pi\left(e^{-\xi}\left(\phi_{,\mu}\phi_{,\nu} - \frac{1}{2}\bar{g}_{\mu\nu}(\phi_{,\rho}\phi^{,\rho})\right)^{;\nu}\right)$$

$$
\begin{aligned}
= \quad & \lambda^{-1}\left(\xi_{,\nu}\xi_{,\mu}{}^{;\nu} + \xi_{,\mu}\bar{\Box}\xi - \xi_{,\rho}\xi_{,\mu}{}^{;\rho}\right) + \\
& 8\pi\left(-e^{-\xi}\xi^{,\nu}\left(\phi_{,\mu}\phi_{,\nu} - \frac{1}{2}\bar{g}_{\mu\nu}\phi_{,\rho}\phi^{,\rho}\right) + e^{-\xi}\bar{\Box}\phi\phi_{,\mu}\right) \qquad (2.44)
\end{aligned}
$$

To continue this check, the equation of motion for the scalar field in the Einstein frame, $\bar{\Box}\psi$, is computed in terms of $\Box\psi$, the Klein-Gordon equation for the scalar field

$$
\begin{aligned}
\Box\psi &= 0 \\
&= \Gamma^{-1}\left(\Gamma g^{\mu\nu}\psi_{,\mu}\right)_{,\nu} \\
&= \phi^2\bar{\Gamma}^{-1}\left(\bar{\Gamma}\phi^{-2}\phi\bar{g}^{\mu\nu}\psi_{,\mu}\right)_{,\nu} \\
&= \phi\bar{\Box}\psi - \phi_{,\nu}\bar{g}^{\mu\nu}\psi_{,\mu} \\
0 &= \bar{\Box}\psi - \bar{g}^{\mu\nu}\xi_{,\nu}\psi_{,\mu} \qquad (2.45)
\end{aligned}
$$

Recalling equation (2.43) along with the above result, the two scalar field equations of motion are

$$
\begin{aligned}
\bar{\Box}\psi &= \bar{g}^{\mu\nu}\xi_{,\mu}\psi_{,\nu} \equiv S \qquad (2.46) \\
\bar{\Box}\xi &= -4\pi\lambda e^{-\xi}\psi^{,\nu}\psi_{,\nu} \equiv S' \qquad (2.47)
\end{aligned}
$$

Using these two equations, the Bianchi identity (2.44) becomes

$$
\bar{G}_{\mu\nu;}{}^{\nu} = 4\pi\xi_{,\mu}\left(\bar{T}_M + e^{-\xi}\psi_{,\rho}\psi^{,\rho}\right) = 0 \qquad (2.48)
$$

which, from equation (2.42) for $\bar{T}_M$, is indeed zero. Thus, the calculated $\bar{G}_{\mu\nu}$ (2.37) is consistent with the Bianchi identities.

For the rest of this chapter, the equations are valid in the Einstein frame, and the use of bars to denote as such is dropped.

2.2.2 Scalar Field Equations

As a matter of convenience and recalling that ψ represents the scalar field while ξ represents the logarithm of the Brans-Dicke field, I introduce the following auxiliary variables

$$\begin{aligned} Q &\equiv \xi' \\ \Phi &\equiv \psi' \\ P &\equiv \frac{a}{\alpha}\left(\dot{\xi} - \beta\xi'\right) \\ \Pi &\equiv \frac{a}{\alpha}\left(\dot{\psi} - \beta\psi'\right) \end{aligned} \tag{2.49}$$

With these defined, some simple quantities become

$$\begin{aligned} \psi^{,t} &= g^{tt}\psi_{,t} + g^{tr}\psi_{,r} \\ &= \left(-\frac{1}{\alpha^2}\right)\left(\frac{\alpha}{a}\Pi + \beta\Phi\right) + \left(\frac{\beta}{\alpha^2}\right)\Phi \\ &= -\frac{\Pi}{\alpha a} \end{aligned} \tag{2.50}$$

$$\begin{aligned} \psi^{,r} &= g^{rr}\psi_{,r} + g^{rt}\psi_{,t} \\ &= \left(\frac{1}{a^2} - \frac{\beta^2}{\alpha^2}\right)(\Phi) + \frac{\beta}{\alpha^2}\left(\frac{\alpha}{a}\Pi + \beta\Phi\right) \\ &= \frac{1}{\alpha a}\left(\frac{\alpha}{a}\Phi + \beta\Pi\right) \end{aligned} \tag{2.51}$$

and also with the scalar field lacking derivatives in θ or ϕ directions because of spherical symmetry

$$\begin{aligned} \psi^{,\mu}\psi_{,\mu} &= \psi^{,t}\psi_{,t} + \psi^{,r}\psi_{,r} \\ &= -\frac{\Pi}{\alpha a}\left(\frac{\alpha}{a}\Phi + \beta\Pi\right) + \left[\frac{1}{\alpha a}\left(\frac{\alpha}{a}\Phi + \beta\Pi\right)\right](\Phi) \end{aligned}$$

$$
\begin{aligned}
&= -\frac{\Pi^2}{a^2} - \frac{\beta}{\alpha a}\Phi\Pi + \frac{\Phi^2}{a^2} + \frac{\beta}{\alpha a}\Phi\Pi \\
\psi^{,\mu}\psi_{,\mu} &= \frac{\Phi^2 - \Pi^2}{a^2}
\end{aligned} \tag{2.52}
$$

Also

$$
\begin{aligned}
g^{\mu\nu}\psi_{,\mu}\xi_{,\nu} &= \psi^{,\nu}\xi_{,\nu} \\
&= \psi^{,r}\xi_{,r} + \psi^{,t}\xi_{,t} \\
&= \left[\frac{1}{\alpha a}\left(\frac{\alpha}{a}\Phi + \beta\Pi\right)\right]Q - \left(\frac{\Pi}{\alpha a}\right)\left(\frac{\alpha}{a}P + \beta Q\right) \\
&= \frac{\Phi Q - \Pi P}{a^2}
\end{aligned} \tag{2.53}
$$

The previous results allow the equations of motion for the two fields to be computed in terms of the introduced auxiliary variables. The equations of motion for both ψ and ξ are defined in terms of general sources S, and S' respectively

$$
\begin{aligned}
\Box\psi &= \Gamma^{-1}\left(\Gamma g^{\mu\nu}\psi_{,\mu}\right)_{,\nu} \\
&= S
\end{aligned} \tag{2.54}
$$

$$
\begin{aligned}
\Box\xi &= \Gamma^{-1}\left(\Gamma g^{\mu\nu}\xi_{,\mu}\right)_{,\nu} \\
&= S'
\end{aligned} \tag{2.55}
$$

where once again $\Gamma \equiv \sqrt{-|g|} = \alpha a r^2 b^2 \sin\theta$. The angular part of the determinate passes through the derivative and thus cancels with its multiplicative inverse. For example, the result for the field ψ is

$$
\begin{aligned}
\dot{\Pi} &= \frac{1}{r^2 b^2}\left(r^2 b^2\left(\beta\Pi + \frac{\alpha}{a}\Phi\right)\right)' + \\
&= 2\left(\alpha K_\theta^\theta - \beta\left(rb\right)^{-1}\left(rb\right)'\right)\Pi - \alpha a S
\end{aligned} \tag{2.56}
$$

$\dot{\Phi}$ can be found by solving algebraically for the time derivative of the field from the defining relation for Π and then taking the spatial derivative. In this manner

$$\dot{\Phi} = \left(\beta\Phi + \frac{\alpha}{a}\Pi\right)' \tag{2.57}$$

With the general form of the solution found, the source terms S and S' must only be found to have the evolution equations for both sets of scalar field variables.

The general equations of motion for the two fields are found in equations (2.46) as

$$\Box\xi = -4\pi\lambda e^{-\xi} g^{\mu\nu}\psi_{,\mu}\psi_{,\nu} \tag{2.58}$$

$$\Box\psi = g^{\mu\nu}\psi_{,\mu}\xi_{,\nu} \tag{2.59}$$

From the general relations (2.56, 2.57) substituting for S, where I have used $b = 1$, $\beta = 0$, and $K^{\theta}_{\theta} = 0$, the variables for both fields become

$$\dot{Q} = \left(\frac{\alpha}{a}P\right)' \tag{2.60}$$

$$\dot{P} = \frac{1}{r^2}\left(\frac{r^2\alpha}{a}Q\right)' + 4\pi\lambda e^{-\xi}\frac{\alpha}{a}\left(\Phi^2 - \Pi^2\right) \tag{2.61}$$

$$\dot{\Phi} = \left(\frac{\alpha}{a}\Pi\right)' \tag{2.62}$$

$$\dot{\Pi} = \frac{1}{r^2}\left(\frac{r^2\alpha}{a}\Phi\right)' + \frac{\alpha}{a}\left(\Pi P - \Phi Q\right) \tag{2.63}$$

These equations, along with those for a and α, determine the evolution of the two fields.

2.2.3 Determining Geometry Equations from Einstein Equations

I have already stated that the solutions for the Brans-Dicke universe can be obtained from the transformations (2.24). Before substituting the new densities ρ_{total} and j^a_{total} into the Einstein equations, these values must be computed.

The densities can be calculated from the defining relations (2.6, 2.7). The stress-energy tensor involved in the definition, however, is that which occurs in the Einstein frame. Relation (2.37) shows that

$$\bar{T}^{BD}_{\mu\nu} = \left(\frac{3+2\omega}{16\pi}\right)\left(\xi_{,\mu}\xi_{,\nu} - \frac{1}{2}\bar{g}_{\mu\nu}\bar{g}^{\rho\sigma}\xi_{,\rho}\xi_{,\sigma}\right) \tag{2.64}$$

which has the same form as that for the scalar field up to a constant.

I compute using the relations

$$\begin{aligned} n^\mu n_\mu &= -1 && (2.65)\\ n_\mu &= (-\alpha, 0, 0, 0) && (2.66)\\ \theta_{,\theta} &= 0 && (2.67)\\ \theta_{,\varphi} &= 0 && (2.68) \end{aligned}$$

Calculating for $\theta = \psi$ or $\theta = \xi$ to within a multiplicative constant gives

$$\begin{aligned} \rho &= n^\mu n^\nu T_{\mu\nu}\\ &= n^\mu n^\nu \left(\theta_{,\mu}\theta_{,\nu} - \frac{1}{2}g_{\mu\nu}g^{\delta\gamma}\theta_{,\delta}\theta_{,\gamma}\right)\\ &= n^\mu n^\nu \theta_{,\mu}\theta_{,\nu} + \frac{1}{2}\theta^{,\delta}\theta_{,\delta}\\ &= \frac{1}{\alpha^2}\theta_{,t}\theta_{,t} + \frac{1}{2}\theta^{,\delta}\theta_{,\delta} \end{aligned} \tag{2.69}$$

so that

$$\rho^{SF} = \frac{\Phi^2 + \Pi^2}{2a^2\phi} \tag{2.70}$$

$$\rho^{BD} = \frac{Q^2 + P^2}{16\pi a^2 \lambda} \tag{2.71}$$

The momentum density must also be calculated. Using the defining relation (2.7), I compute, again for the general field, θ

$$\begin{aligned} j^i_\psi &= g^{ik} j_k \\ &= -g^{ik} n_\mu T^\mu_k \end{aligned} \tag{2.72}$$

Clearly, terms appearing in (2.72) with $\mu \neq t$ vanish so that j^r for the scalar field becomes

$$\begin{aligned} j^r_\psi &= -\phi^{-1} n_t \psi^{,r} \psi^{,t} \\ &= e^{-\xi} \alpha \left(\frac{\Phi}{a^2}\right)\left(\frac{-\Pi}{\alpha a}\right) \\ &= \frac{-\Phi\Pi}{e^\xi a^3} \end{aligned} \tag{2.73}$$

and

$$j_r = \frac{-\Phi\Pi}{e^\xi a} \tag{2.74}$$

With these results, the Hamiltonian constraint (2.11) in the polar/radial scheme is

$$\frac{a'}{a} + \frac{a^2 - 1}{2r} = 4\pi r a^2 \rho \tag{2.75}$$

which, with the two energy density terms (2.70, 2.71), becomes

$$\frac{a'}{a} + \frac{a^2 - 1}{2r} = 4\pi r a^2 \left[\frac{\Phi^2 + \Pi^2}{2a^2 e^\xi} + \frac{1}{16\pi\lambda a^2}\left(Q^2 + P^2\right)\right] \tag{2.76}$$

Again from Choptuik [Choptuik,1986], the surviving momentum constraint (2.12) in the polar/radial scheme is

$$K_r^r = -4\pi r j_r \tag{2.77}$$

which given (2.74) is

$$K_r^r = \frac{4\pi r}{a}\left(e^{-\xi}\Phi\Pi + \frac{1}{8\pi\lambda}QP\right) \tag{2.78}$$

The slicing constraint is dependent only on geometry, and therefore remains the same as for the Einstein case. That this constraint does not involve the matter variables is a special feature of the polar/radial scheme [Choptuik,1986]

$$\alpha' + \left(\frac{1-a^2}{r} - \frac{a'}{a}\right)\alpha = 0 \tag{2.79}$$

From the evolution equations (2.13) the evolution equation for the metric function a can be found as

$$\dot{a} = -\alpha a K_r^r \tag{2.80}$$

Though not needed by the code to evolve the fields, the time evolution of the extrinsic curvature is found from (2.14) which computes to

$$\dot{K}_r^r = -\frac{1}{a}\left(\frac{\alpha'}{a}\right)' + \alpha\left(-\frac{2}{ra}\left(\frac{1}{a}\right)' + K_r^{r2} - \frac{8\pi}{a^2}\left(e^{-\xi}\Phi^2 + \frac{1}{8\pi\lambda}Q^2\right)\right) \tag{2.81}$$

In summary, the equations derived in this section for the geometry are

$$\alpha' = -\left(\frac{1-a^2}{r} - \frac{a'}{a}\right)\alpha \tag{2.82}$$

$$a' + \frac{a^3 - a}{2r} = 2\pi a r \left(e^{-\xi} \left(\Phi^2 + \Pi^2 \right) + \frac{1}{8\pi\lambda} \left(Q^2 + P^2 \right) \right) \quad (2.83)$$

$$K_r^r = \frac{4\pi r}{a} \left(e^{-\xi} \Phi\Pi + \frac{1}{8\pi\lambda} QP \right) \quad (2.84)$$

$$\dot{a} = -\alpha a K_r^r \quad (2.85)$$

$$\dot{K}_r^r + \frac{1}{a} \left(\frac{\alpha'}{a} \right)' = \alpha \left(-\frac{2}{ra} \left(\frac{1}{a} \right)' + K_r^{r2} - \frac{8\pi}{a^2} \left(e^{-\xi} \Phi^2 + \frac{1}{8\pi\lambda} Q^2 \right) \right) \quad (2.86)$$

Along with equations (2.60 - 2.63), these determine the entire model.

2.3 Evolution Scheme

Equipped with the necessary equations, determining analytic solutions appears quite daunting, if possible at all. Instead, the solutions are found using computational methods. The idea involved is to determine initial data consistent with the constraints of the equations and evolve that data using finite differences [Choptuik,1986].

In a time dependent simulation, initial data is specified, and then, armed with equations specifying the evolution, the data is evolved. A problem present with the 3+1 formalism, is that the initial data are not freely specifiable because they are constrained by certain of the field equations. However, with the scheme used, the profiles of the scalar fields can be freely specified, and then the geometry is computed consistent with the constraints.

With the all the initial data determined, the evolution is governed by the equations for the time derivatives of the fields. For example, given some field $\theta(x^i, t = 0) = \theta_0(x^i)$ specified at the initial time whose equation of motion specifies the time derivative of θ as some function, L, of space, time, and other

fields as

$$\frac{d\theta}{dt} = L(\theta, x^i, t, \ldots) \tag{2.87}$$

the profile of θ at some later time is simply

$$\theta(x^i, t + dt) = \theta(x^i, t) + L\, dt \tag{2.88}$$

Continually applying (2.88) will evolve θ through time. Computationally, it is necessary to express dt as some small quantity Δt instead of an infinitesimal quantity. This method of approximating differentials as finite differences is appropriately called *finite differencing* and is discussed in the following section[Choptuik,1986].

Once the fields in this problem are evolved one unit of Δt, the geometric variables a and α are then updated via the constraint equations (2.83) and (2.82) using finite differences for the spatial derivatives.

The data that initially need to be provided here are the values of the scalar fields, ψ and ϕ. These are freely specifiable, and in general throughout this thesis, I pick a Gaussian pulse of the form

$$\theta = A \exp\left[-\left(\frac{r - R_\theta}{\Delta}\right)^2\right] \tag{2.89}$$

with R_θ, A, and Δ constants defining the initial shape of the pulse. In addition to these fields at the initial time, the functions a, and α must be computed to evolve the system. However, these two functions are determined once the scalar fields have been specified from the geometric equations found in Section 2.2.2.

In order to finite difference, the domain over which the functions are defined, $0 \leq r \leq R$, must be discretized. With some arbitrary maximum, R,

the domain, now called a 1-dimensional *grid* or *mesh*, is constructed according to

$$r_j = jh \;\Rightarrow\; j = 0 \ldots J \tag{2.90}$$

with $h = R/J$ and $J + 1$ is the number of points in the grid. Time is likewise discretized where discrete times are denoted by

$$t^n = n\Delta t \;\Rightarrow\; n = 0 \ldots N \tag{2.91}$$

Choosing a Gaussian pulse for the initial configuration of both fields, ψ and ξ are given values at the discrete points in the mesh

$$\begin{aligned} \psi &= A_M \exp\left[\left(\frac{r_j - R_M}{\Delta_M}\right)^2\right] \\ \xi &= A_{BD} \exp\left[\left(\frac{r_j - R_{BD}}{\Delta_{BD}}\right)^2\right] \end{aligned} \tag{2.92}$$

where A is a parameter specifying the amplitude of the pulse, and Δ the width. The value of R specifies the initial position of the peak of the pulse. The associated derivatives of these two fields, Φ, Π, P, Q, are similarly be initialized.

At this point, exact initial data, sampled at regular intervals in the continuum, have been placed in storage as arrays. The finite differencing takes these data and evolves them. Again, for an arbitrary field $\theta(x^i, t)$, the corresponding grid function, $\hat{\theta}$, could be computationally evolved via equation (2.88) with the replacement of differentials with finite differences

$$\hat{\theta}(r_j, t^{n+1} = t^n + \Delta t) = \hat{\theta}(r_j, t^n) + \Delta t \left[\frac{d\hat{\theta}}{dt}\right] \tag{2.93}$$

Given some data determined at some time $t^n = n\Delta t$ and some evolution equation for $d\hat{\theta}/dt$, the field at time t^{n+1} can be computed. Work done here uses a

modified form (2.93) in which differencing is performed around $\theta(r_j, t^n)$ as

$$\hat{\theta}(r_j, t^{n+1}) = \hat{\theta}(r_j, t^{n-1}) + 2\Delta t \left[\frac{d\hat{\theta}}{dt}\right] \tag{2.94}$$

which is discussed in Section 2.3.1.

Recall that the constructed universe contains two dynamic fields, one the massless scalar field representing some initial mass-energy, ψ, and one the Brans-Dicke field representing the variations of the gravitational constant, $\phi \equiv e^{\xi}$. The constraint equations specify, however, constraints on the structure of the universe with respect to the mass distribution. Thus, they apply at the initial time and at all subsequent times. The constraints here serve to completely determine the initial form of the metric once the dynamic fields have been specified. With the simplification provided by the polar/radial scheme, solving for the two metric functions a and α yields the entire four-metric ${}^{(4)}g_{\mu\nu}$.

The metric function a depends only on the source terms of the fields, those being the derivatives Π, Φ, P, and Q, as is shown in Section 2.2.2. This equation is solved using a pointwise Newton method. With this method, I solve the Hamiltonian constraint (2.83) which has the form

$$H(a, a') = a' + f(a) + g(\ldots) = 0 \tag{2.95}$$

for some functions $H(a, a')$, $f(a)$, and $g()$, which is independent of a. Centered differencing this around $a_{j+1/2}$ provides

$$\hat{H} = \frac{a_{j+1} - a_j}{h} + \hat{f}\left(\frac{1}{2}\left(a_j + a_{j+1}\right)\right) + \hat{g}(\ldots) = 0 \tag{2.96}$$

The above equation is then solved for every a_{j+1}. One begins with some guess $a_{j+1}^{(0)}$ where the mth iteration provides the value $a_{j+1}^{(m)}$. The iterative process

$$a_{j+1}^{(m+1)} = a_{j+1}^{(m)} - \delta a_{j+1}^{(m)} \tag{2.97}$$

obtains successive approximations to the differential equation (2.96). The correction factor $\delta a_{j+1}^{(m)}$ is described according to the procedure as

$$\delta a_{j+1}^{(m)} = \frac{H^{(m)}}{\partial H^{(m)}/\partial a_{j+1} \mid_{a_{j+1}^{(m)}}} \tag{2.98}$$

where $H^{(m)}$ is the *residual* whose value approaches zero for a convergent scheme. This process is iterated on m until the residual is below some threshold. The process begins again for $j+2$ where the initial guess is extrapolated from the previous two results

$$a_{j+2}^{(0)} = 2a_{j+1} - a_j \tag{2.99}$$

In this manner, at every time step t^n, the values of a_j^n for all j are found.

The final function for which one must solve is the lapse function, $\alpha(r,t)$. As discussed previously, this is the function which measures the lapse in time between slices. Since r and t parameterize the universe and with the shift $\beta = 0$, when $\alpha = 1$, t represents proper time. This is because proper time T is determined by integrating the metric between two points spread in time yielding

$$T(r,t) = \int_0^t \alpha(r,t)d\tilde{t} \tag{2.100}$$

Introducing $T_0 \equiv T(r=0,t) =$ central proper time, the slices could be labeled, instead of with the coordinate t, with this central proper time. Because

$$T_0 = \int_0^t \alpha(0,t)d\tilde{t} \tag{2.101}$$

setting $\alpha(r=0,t) = 1$ would re-label each slice with the central proper time.

The idea behind the slicing is that near the developing singularity $\alpha \to 0$. Thus proper time proceeds extremely slowly, effectively freezing the

evolution near the singularity. This avoids the complications when indeed it becomes a singularity. The evolution equation for α is simply an ordinary differential equation which is solved for α in terms of a, again using second order finite difference techniques.

2.3.1 Finite Differencing

The previous section details the general method by which the initial data is found and evolved. However, given some constraint or evolution equation, it must be expressed in terms of small differences as opposed to the infinitesimal differentials. The differential can be approximated as

$$\frac{\partial}{\partial x}u(x) \Rightarrow \frac{\hat{u}(x_j) - \hat{u}(x_{j-1})}{x_j - x_{j-1}} = \frac{\hat{u}_j - \hat{u}_{j-1}}{h} \tag{2.102}$$

where $x_j - x_{j-1} = h$ and $\hat{u}_j = \hat{u}(x_j)$. Notice here, the analytic function $u(x)$ has no hat, while the finite differenced $\hat{u}$ has values only for $x_j = jh$. Again, variables with hats represent function defined on the grid, whereas those without represent continuum solutions. This construction is called *backward differencing* because it approximates the differential with respect to change from the previous (hence backwards) value. We could have similarly *forward differenced* $u(x)$.

This is all well and good, but one may wonder how accurate such an approximation is. By Taylor expanding the arbitrary function $u(x-h)$ around x and using a prime to denote $\partial/\partial x$

$$u(x-h) = u(x) - u'h + \frac{1}{2}u''h^2 - \frac{1}{6}u'''h^3 + \ldots \tag{2.103}$$

Solving for u' in terms of the backwards difference seen in equation (2.102)

$$u' = \frac{u(x-h) - u(x)}{h} - \frac{1}{2}u''h + \frac{1}{6}u'''h^2 + \ldots \tag{2.104}$$

and thus the backwards difference has error terms shown in brackets below

$$\frac{u(x-h) - u(x)}{h} = u' + \left[-\frac{1}{2}u''h + \frac{1}{6}u'''h^2 + \ldots\right] \tag{2.105}$$

which means that backward differencing is $O(h)$. This error, the truncation error, is defined explicitly in the following section.

Forward differencing yields the similar equation

$$u(x+h) = u(x) + u'h + \frac{1}{2}u''h^2 + \frac{1}{6}u'''h^3 + \ldots \tag{2.106}$$

which is also $O(h)$. Consider, however, the result of subtracting equation (2.103) from equation (2.106):

$$u(x+h) - u(x-h) = 2u'h + 2\frac{1}{6}u'''h^3 + \ldots \tag{2.107}$$

yielding a *center differenced* approximation for u'

$$u' = \frac{u(x+h) - u(x-h)}{2h} + O(h^2) \tag{2.108}$$

The above shows that center-differencing has an error term $O(h^2)$ and is thus termed a second order difference scheme.

With this formalism in hand, we re-express the determining equations found in Section 2.2.2 in terms of second order, center-differences as:

$$\Phi_j^{n+1} = \Phi_j^{n-1} + \frac{\Delta t}{h}\left[\frac{\alpha_{j+1}^n \Pi_{j+1}^n}{a_{j+1}^n} - \frac{\alpha_{j-1}^n \Pi_{j-1}^n}{a_{j-1}^n}\right] \tag{2.109}$$

$$\Pi_j^{n+1} = \Pi_j^{n-1} + \frac{6\Delta t}{r_{j+1}^3 - r_{j-1}^3}\left[\frac{(r_{j+1}^n)^2\alpha_{j+1}^n}{a_{j+1}^n}\Phi_{j+1}^n - \frac{(r_{j-1}^n)^2\alpha_{j-1}^n}{a_{j-1}^n}\Phi_{j-1}^n\right] + \frac{\alpha_j^n}{a_j^n}\left(\Pi_j^n P_j^n - \Phi_j^n Q_j^n\right) \quad (2.110)$$

$$Q_j^{n+1} = Q_j^{n-1} + \frac{\Delta t}{h}\left[\frac{\alpha_{j+1}^n P_{j+1}^n}{a_{j+1}^n} - \frac{\alpha_{j-1}^n P_{j-1}^n}{a_{j-1}^n}\right] \quad (2.111)$$

$$P_j^{n+1} = P_j^{n-1} + \frac{6\Delta t}{r_{j+1}^3 - r_{j-1}^3}\left[\frac{(r_{j+1}^n)^2\alpha_{j+1}^n}{a_{j+1}^n}Q_{j+1}^n - \frac{(r_{j-1}^n)^2\alpha_{j-1}^n}{a_{j-1}^n}Q_{j-1}^n\right] + 4\pi\lambda e^{-\xi_j^n}\frac{\alpha_j^n}{a_j^n}\left(\Phi_j^{n2} + \Pi_j^{n2}\right) \quad (2.112)$$

where Δt is the finite increment in time taken. Here I am using the notation such that X_j^n indicates the value of the function at $r = jh$ and $t = n\Delta t$.

Because the equations are hyperbolic, gradients in the spatial dimensions are the same magnitude as those in time. Hence, setting the spatial resolution roughly equal to that attained in time is the logical approach. I let σ denote the ratio between the two via $\sigma = \Delta t/h$. Whenever a series of computations is performed using the same initial data, but different resolutions, *sigma* is kept constant. Because of stability issues discussed in [Choptuik,1986], σ should be strictly less than unity.

2.3.2 Richardson Expansion

The previous section shows how finite differencing takes operators such as $\partial f/\partial x \Rightarrow (f_{j+1} - f_{j-1})/(2h)$. Work by Richardson [Richardson,1910] called *Richardson Expansion* examines the error involved in finite differencing [Choptuik,1986].

Given some differential equation of a function u in terms of a general

differential operator L expressed as

$$Lu = 0 \tag{2.113}$$

a finite difference approximation in terms of the finite difference operator $\hat{L}$ and the solution $\hat{u}$ becomes

$$\hat{L}\hat{u} = 0 \tag{2.114}$$

Equation (2.114) represents the approximation to (2.113), though $\hat{L}\hat{u}$ is exactly equal to 0. The error in the difference operator $\hat{L}$ is called the *truncation error*, $\hat{\tau}$ and is defined in terms of the difference operator and the exact solution as

$$\hat{\tau} \equiv \hat{L}u \tag{2.115}$$

With this definition, recalling equation (2.105) one can see that this definition leads to the bracketed term being the truncation error.

Likewise, we have the *solution error* $\hat{e}$ defined as

$$\hat{e} \equiv u - \hat{u} \tag{2.116}$$

As discussed in the above section, these error terms are said to be m order accurate if $\hat{\tau} = O(h^m)$ and if $\hat{e} = O(h^m)$. Clearly, we intuitively assume both error terms to be of the same order in which case the scheme is said to be *optimally convergent*. Choptuik in [Choptuik,1991] argues that schemes such as those used here are indeed optimally convergent.

For the cases at hand for which the exact solution is unknown, the truncation error, $\hat{\tau}$, is unknown as well because its computation necessitates the exact solution u. In an effort to measure this error, Richardson makes

the assumption based on reasoning discussed in the previous section, that the differenced solution $\hat{u}_j$ can be expanded in terms of the exact solution and error functions e_i (assuming solutions of $O(h^2)$) [Richardson,1910]

$$\hat{u}_j = u(x) + h^2 e_2(x) + \ldots \tag{2.117}$$

This analysis can then be used to test convergence of the solutions. With solutions $\hat{u}_h$, $\hat{u}_{2h}$, and $\hat{u}_{4h}$, the differences using equation (2.117) appear

$$\begin{aligned} \hat{u}_{2h} - \hat{u}_h &= 4h^2 - h^2 \\ \hat{u}_{4h} - \hat{u}_{2h} &= 16h^2 - 4h^2 \end{aligned} \tag{2.118}$$

Thus, after completion of the modeling code, taking solutions at the three discretization levels of h, $2h$, and $4h$, a researcher can compute the *convergence factor*

$$\frac{\hat{u}_{2h} - \hat{u}_h}{\hat{u}_{4h} - \hat{u}_{2h}} \tag{2.119}$$

which should, for $O(h^2)$ solutions, converge to the value 1/4.

2.3.3 Boundary Conditions

Since centered differencing of wave equations of the form found in (2.109 - 2.112) requires values both to the left and the right of the destination value, one must determine appropriate edge conditions for the scalar fields. With these boundary conditions, I may specify the values of the quantities to be evolved at each of the boundaries, while using difference equations to solve the interior (see [Choptuik,1994] pg. 2-3).

The following boundary conditions apply for either scalar field. Thus, the discussion uses θ to represent either ψ or ξ. Near the origin, θ is assumed

regular such that

$$\lim_{r\to 0}\theta(r,t) = \theta_0(t) + r^2\theta_2(t) + \ldots \tag{2.120}$$

which shows that near the inner boundary

$$\Phi \equiv \theta' = 2r\theta_2(t) + \ldots \tag{2.121}$$

which, at the inner boundary $r = 0$, yields $\Phi = 0$.

Similarly, the temporal derivative at the origin is found using a second order quadratic fit. Specifically, with

$$\Pi = f_0(t) + r^2 f_2(t) + \ldots \tag{2.122}$$

the first three values of the field at $r = 0, h, 2h$ are to second order

$$\begin{aligned} \Pi_{r=0} &= f_0(t) \\ \Pi_{r=h} &= f_0(t) + h^2 f_2(t) \\ \Pi_{r=2h} &= f_0(t) + (2h)^2 f_2(t) \end{aligned} \tag{2.123}$$

Solving the system of equations (2.123), yields the condition

$$\Pi_{r=0} = f_0(t) = \frac{4\Pi_{r=h} - \Pi_{r=2h}}{3} \tag{2.124}$$

The outer boundary condition assumes that no energy is coming from $r > R$ and that the geometry near $r = R$ is almost flat. Thus, $r\theta$ near the outer boundary is a function of $(r - t)$

$$\lim_{r\to\infty} r\theta(r,t) = f(r-t) \tag{2.125}$$

which implies that

$$\begin{aligned} \frac{\partial(r\theta)}{\partial t} &= \frac{\partial f(r-t)}{\partial t} \\ \frac{\partial(r\theta)}{\partial r} &= \frac{\partial f(r-t)}{\partial r} \end{aligned} \tag{2.126}$$

Since $\partial f(r-t)/\partial t = -\partial f(r-t)/\partial r$

$$\lim_{r\to\infty} \frac{\partial\theta}{\partial t} + \frac{\partial\theta}{\partial r} + \frac{\theta}{r} = 0 \tag{2.127}$$

With this result, I take separately the time and space derivatives yielding

$$\begin{aligned} \lim_{r\to\infty} \frac{\partial\pi}{\partial t} + \frac{\partial\pi}{\partial r} + \frac{\pi}{r} &= 0 \\ \lim_{r\to\infty} \frac{\partial\Phi}{\partial t} + \frac{\partial\Phi}{\partial r} + \frac{\Phi}{r} - \frac{\theta}{r^2} &= 0 \end{aligned} \tag{2.128}$$

The above results (2.128) become after second order backwards differencing and neglecting terms of $O(r^{-2})$[Choptuik,1994]

$$\Phi_J^{n+1} = \left(\frac{3}{\Delta t} + \frac{3}{h} + \frac{2}{r_J}\right)^{-1} \left(\frac{4\Phi_J^n - \Phi_J^{n-1}}{\Delta t} + \frac{4\Phi_{J-1}^{n+1} - \Phi_{J-2}^{n+1}}{h}\right) \tag{2.129}$$

$$\Pi_J^{n+1} = \left(\frac{3}{\Delta t} + \frac{3}{h} + \frac{2}{r_J}\right)^{-1} \left(\frac{4\Pi_J^n - \Pi_J^{n-1}}{\Delta t} + \frac{4\Pi_{J-1}^{n+1} - \Pi_{J-2}^{n+1}}{h}\right) \tag{2.130}$$

where $r_J = R$ is the outermost grid point.

2.4 Adaptive Mesh Refinement

As mentioned previously, the error in these numerical results is expected to be of the order of the square of the mesh spacing. Thus, for every halving of the mesh spacing, the error should drop to a fourth its previous value. For the extreme gradients involved in the non-linear regimes encountered, a fine grid is invaluable. In the non-linear regime encountered by

Choptuik[Choptuik,1993], the detail occurs at scales that shrink exponentially in both time and space.

With a single grid of uniform mesh spacing, a tremendous amount of overhead is incurred by maintaining a fine grid for large radii where no sharp gradients occur. The computation time involved in solving such an over-refined grid is very long. In addition, the memory necessary to store such a tremendous amount of data is enormous.

However, Berger and Oliger [Berger,1984] have outlined a method by which the grid is dynamically adapted such that the resolution is provided only where necessary. Choptuik[Choptuik,1994] has implemented the algorithm in spherical symmetry. In this scheme, the algorithm, after determining where and when a new grid is necessary, constructs one of an appropriate length. The algorithm recurses up to some maximum resolution, such that the fine grids are nested inside coarser grids.

Upon each of these grids, the evolution routines are called solving for the updated fields. Since the fine grid boundaries are, in general, not physical boundaries, the evolution routines are passed the values at the boundaries found via interpolation in the next coarsest grid, called the parent grid. The evolution and constraint equations are then solved on this fine grid.

A crucial element of the adaptive-mesh technique, is the determination of when a new grid is needed. Berger and Oliger's idea is to create a new grid when the truncation error exceeds some threshold. Since the truncation error is unknown, an approximation technique is needed. In Section 2.3.2, I outline a method by which two solutions are found on two mesh spacings and

subtracted. This same method can be applied on the same grid by simply using values on the same grid spaced $2h$ apart. Thus, for some grid evolution operator Q, which advances the solution from t^n to t^{n+1}, the truncation error at point j can be estimated by

$$\tau_j = Q_j^h Q_j^h - Q_j^{2h} \tag{2.131}$$

where, for the smaller grid of spacing h, the evolution is applied twice and where Q^{2h} is computed as a center-difference around j using the values at $j+2$ and $j-2$. Because the coarse step has a mesh spacing twice that of the fine grid and because on each grid $\Delta t = \sigma h$, the step Q_j^{2h} takes a time step of $2\Delta t$. For that reason, the evolution operator Q_j^h is applied twice before the values obtained are compared.

Chapter 3

Results

Because of the conformal transformation which took the Brans-Dicke equations into the Einstein frame, the fields involved in the evolution can be interpreted very much like those in the general relativistic case. In this frame, mass varies according to the Brans-Dicke field, while the gravitational constant remains fixed. This behavior is in contrast to the canonical Brans-Dicke frame in which rest masses remain constant while the gravitational constant varies [Scheel,1995b]. As such, the evolutions show the two fields, one the Klein-Gordon field and the other the Brans-Dicke field, traveling in the computational domain. The ingoing component of each field travels towards $r = 0$ at which point it explodes through the origin and travels outwards. If a black hole forms, some of the field, and hence its mass, remains near the origin. In the case of black hole formation, one observes mass leaving the domain until a steady state is reached in which some portion of the mass, M_{BH} remains in the region enclosed by the black hole radius, R_{BH}. This mass is that of the black hole formed. Where no hole forms, all the mass leaves the computational domain.

In general relativity, the general spherically symmetric, static solution to the field equations is the Schwarzschild solution with the metric

$$ds^2 = -\left(1 - \frac{2m}{r}\right) dt^2 + \left(1 - \frac{2m}{r}\right)^{-1} dr^2 + d\Omega^2 \tag{3.1}$$

Because the evolution takes place in the Einstein frame, the components of the metric used here

$$ds^2 = -\alpha^2 dt^2 + a^2 dr^2 + d\Omega^2 \tag{3.2}$$

associate themselves with the corresponding Schwarzschild components as

$$\alpha^2 = \left(1 - \frac{2m}{r}\right) \tag{3.3}$$

$$a^2 = \left(1 - \frac{2m}{r}\right)^{-1} \tag{3.4}$$

With this association, the mass aspect function, $m(r,t)$ can be defined such that it represents the amount of mass within some radius r at time t as

$$m(r,t) = \frac{r}{2}\left(1 - a^{-2}\right) \tag{3.5}$$

by which the derivative of the mass becomes

$$\begin{aligned} \frac{dm}{dr} &= \frac{1}{2}\left(1 - a^{-2}\right) + \frac{r}{2}\left(-2a^{-3}a'\right) \\ &= \frac{ra'}{a^3} + \frac{a^2 - 1}{2a^2} \end{aligned} \tag{3.6}$$

Using the Hamiltonian constraint (2.75), this becomes

$$\frac{dm}{dr} = 4\pi r^2 \rho \tag{3.7}$$

With the mass known from equation (3.5), black hole formation is signaled by $2m/r \to 1$. Though the solution is singular for $2m/r = 1$, a sufficiently high threshold value such as 0.995 will not only signal a black hole, but from the location of this formation, the mass can be approximately determined as $M_{BH} = R_{BH}/2$. The black hole is further signaled by the behavior of the mass. After its formation, while most of the mass travels out of the domain, some mass remains in some sphere of radius R_{BH} centered at the origin.

3.1 `bd` Results

Initially I wrote a non-adaptive code, `bd`, to test the difference equations. In this code, I include routines to update the various variables which can then be utilized by the adaptive code. The adaptive code was generated with the invaluable assistance of Matthew Choptuik by converting his adaptive code previously used for the general relativistic equations to the Brans-Dicke equations in the Einstein frame.

With the non-adaptive code, the lack of resolution involved in a uniform mesh prevents any significant measurements from being taken. Instead, the code allows for the easy testing and development of the routines. These routines, once developed, were used in the adaptive code.

A valuable test of the evolution scheme is mass conservation. Evidence of mass coming in from $r = \infty$ would certainly show something wrong with the boundary conditions. In addition, while mass is not leaving the domain, the mass at the boundary should remain constant.

In figure 3.1, I display the mass aspect function at the outer boundary obtained from the metric function a as defined in equation (3.5). The data was computed with 1024 grid points in the computational domain. These values display the amount of mass contained within the entire domain. As shown, it stays essentially constant at a value of $m = 0.0033$ until time $t \approx 33$ (see inset of figure 3.1). At that time the energy associated with the waves has bounced through the origin and is now leaving the domain for $33 \leq t \leq 75$. For $t > 80$, the mass ≈ 0 and it is clear that no black hole has formed.

In Section 2.3.1, I claimed that the finite differencing scheme was

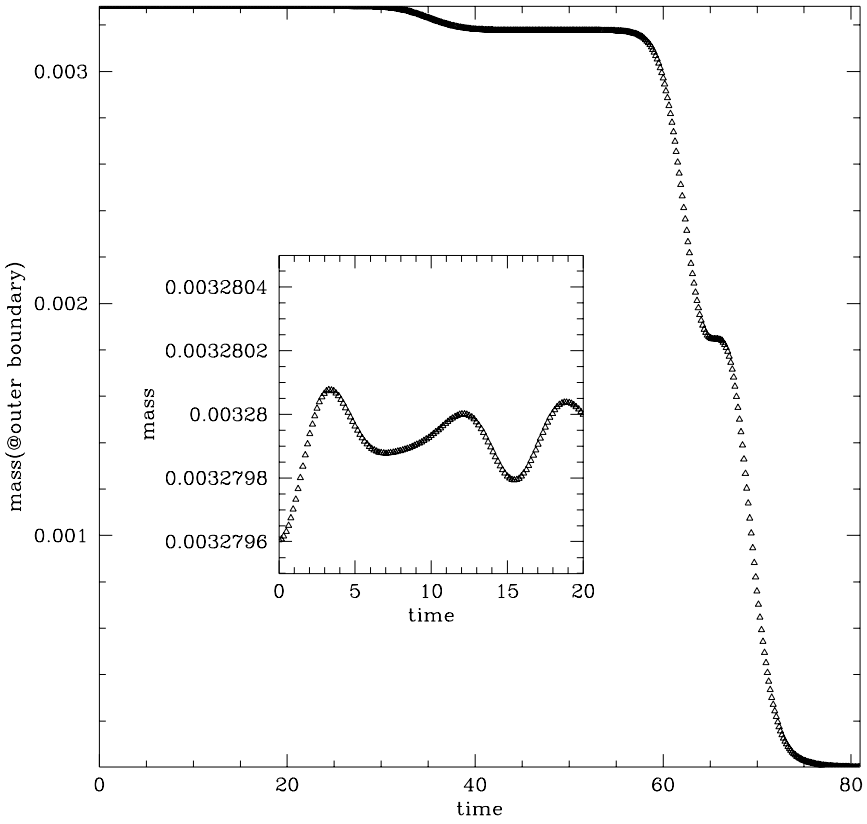

Figure 3.1: Demonstration of mass conservation for a grid of 1024 points

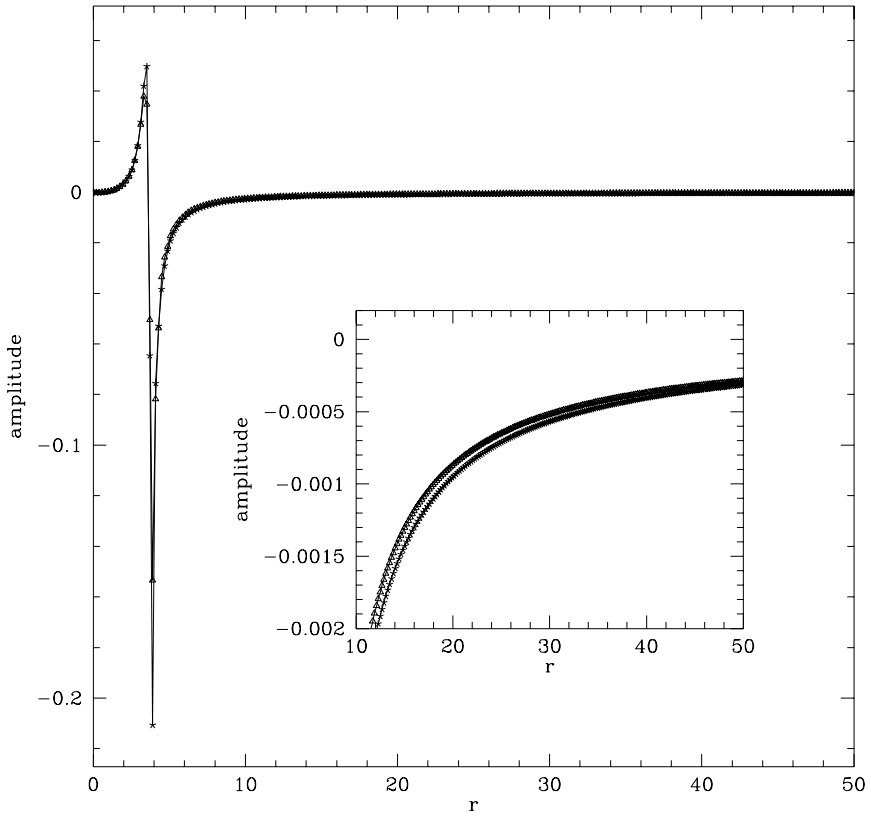

Figure 3.2: Demonstration of second order convergence

second order in the mesh spacing. As a test of this claim, I compute the convergence factors for the various fields as discussed in Section 2.3.2. If the code is run at three mesh spacings of $h, 2h$, and $4h$, then the difference $a_h - a_{2h}$ should be one fourth the magnitude of the difference $a_{2h} - a_{4h}$. Figure 3.2 displays $4\,(a_h - a_{2h})$ and $a_h - a_{2h}$ at a late time $t \approx 30$.

That the profiles in figure 3.2 overlap so well, demonstrates that the calculation of the metric function a is indeed second order. Because of the

coupling of all the variables, the whole scheme would appear second order as well. However, I also tested all other fields with equally convincing results.

As another example of the second order convergence, in the weak field regime, the convergence factor for the metric function a is shown in figure 3.3. The data is computed from three runs with 512, 1024, and 2048 points covering the same domain with decreasing mesh spacing h. The data were obtained by taking the norm of the profiles of $a_{4h} - a_{2h}$ and $a_h - a_{2h}$ at times t and dividing. The l_2 norm was used whereby $l_2|x^n| = \left[\Sigma_{j=0}^{J}(x_j^n)^2/J\right]^{1/2}$. The theoretical constant value of 4 represents perfect second order. The deviations from this value are quite small in the figure.

For runs forming a black hole, the lapse function α is observed to rapidly approach 0 in the central region. Since the proper time is determined from α via equation (2.100), the approach of $\alpha \to 0$ signifies a freezing of the evolution in that region. The slicing conditions of the polar/radial scheme enables the code to avoid a singularity and continue its computation. However, a coordinate singularity at $r = 2M_{BH}$ is approached making the scheme far from ideal for long-term black hole evaluations.

3.2 `bdad` Results

`bdad` is the executable produced by integrating the evolution routines of the Brans-Dicke variables with the adaptive code of Choptuik [Choptuik,1994]. Without the resolution afforded by the adaptive code, accurate observations of black hole mass scaling and scale-periodic behavior would have been impossible.

Using the adaptive code `bdad`, a binary search was conducted on the

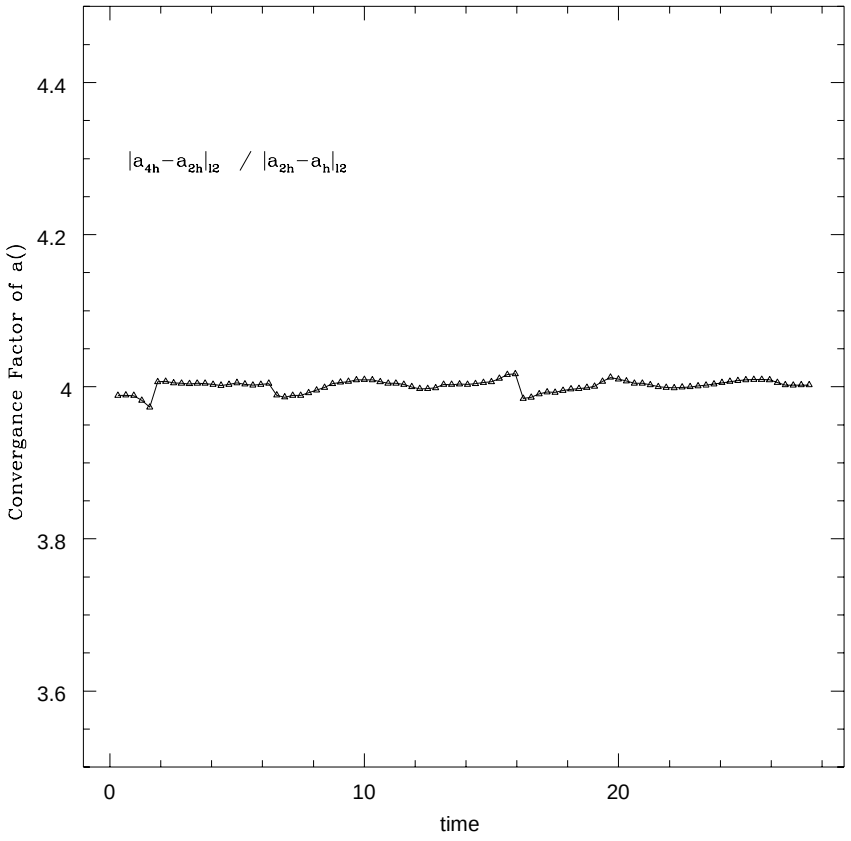

Figure 3.3: Convergence factor for metric function a

amplitude of the initial Brans-Dicke field pulse, while letting the scalar field be zero. Here, I let $\omega = 1$, a regime in which the scalar field couples significantly with the gravitational fields. In contrast, as $\omega \to \infty$, Brans-Dicke solutions satisfy Einstein's field equations.

With a Gaussian shape described by

$$\xi = \xi_o \exp\left[\left(\frac{r - R_o}{\Delta}\right)^q\right] \tag{3.8}$$

the critical value of ξ_o for $\Delta = 3$, $R_o = 20$, and $q = 2$, was $p^* = 0.0543\cdots$. The search on p narrowed the value of p^* down to machine precision such that any value larger than p^* formed a black hole, while all others did not. By taking linear steps in $\ln|p - p^*|$, and finding the mass of the black hole formed for each p, a relation can be found for the black hole mass scaling. The points are shown in figure 3.4. The slope is given by γ, such that

$$M_{bh} = c_i|p - p^*|^\gamma \tag{3.9}$$

where c_i is some constant dependent on the initial pulse. The results indicate that the relation (3.9) holds with $\gamma = 0.37$. These results are identical to those found by Choptuik for the scalar field result [Choptuik,1993].

Further, for this example, near the critical point, scaling such as that found by Choptuik [Choptuik,1993] was found. For the near critical regime, form invariant quantities such as dm/dr were seen to echo. Patterns were traced out on ever decreasing scales. Given some profile of a quantity at the central proper time T_0, the profile of the same quantity some time e^{Δ_t} later on a scale e^{Δ_r} smaller will be identical for a region near the center.

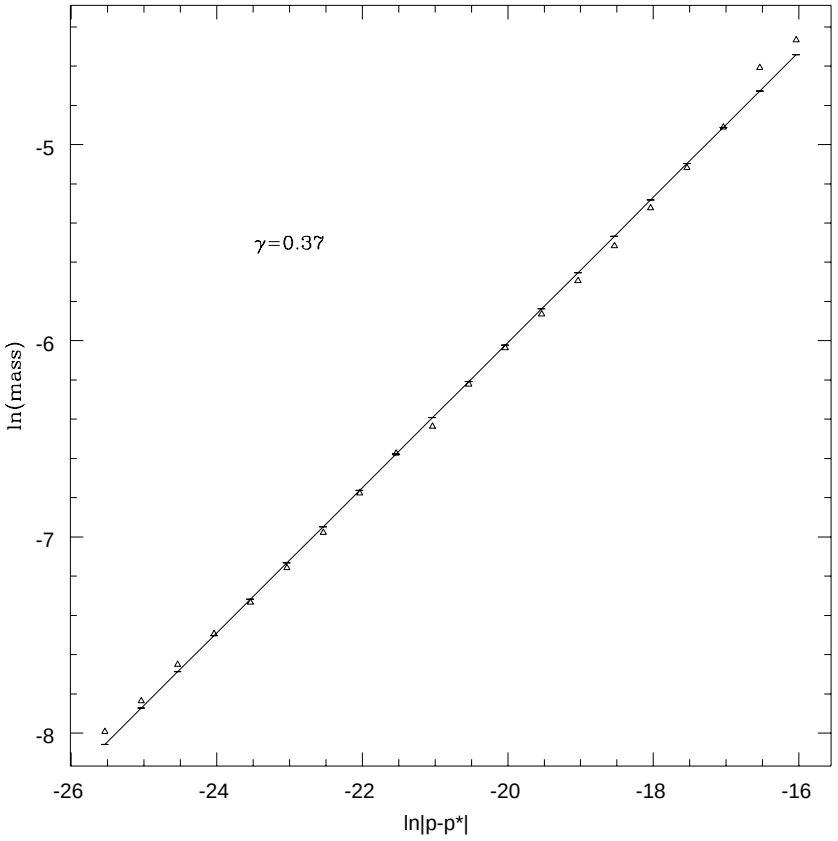

Figure 3.4: Mass scaling for pure Brans-Dicke run ($\gamma = 0.37$)

Figure 3.5 shows three profiles of dm/dr for the near critical regime with just a Brans-Dicke field, and $\omega = 1$. The squares represent the profile at time $t = 36.75695$. The circles display the profile at a later time of $t = 37.6188561$ on a scale such that $r \to re^{3.37}$, where the exponent was determined by visually minimizing discrepancy in the profiles. The last profile occurs at $t = 37.6666221$ with its radius undergoing $r \to re^{6.74}$. All three of the profiles are seen to overlap in all regions excluding the initial hump. Presumably, the first hump is not in the completely non-linear regime and can be discounted. However, all echoing proceeding the initial one, coincide remarkably well.

Choptuik [Choptuik,1993] finds that r scales as $r \to re^{3.44}$ while central proper time rescales as $T \to T + e^{3.43}$. Here, I have found that $r \to re^{3.37}$ which agrees favorably. The discrepancy appears to arise due to fitting the data after the evolution instead of during the evolution, as Choptuik does. After the evolution, the echos have traveled some distance and the fit is less precise than if done at times during the evolution. I was unable to find Δ_τ for this case because the code does not yet maintain the proper time. However, given the three times listed above, it is quite apparent that the structure is repeating on decreasing time scales.

3.3 Brans-Dicke Considerations

The results previously discussed have all been in the Einstein frame. This frame is so constructed as to make the gravitational constant an actual constant while masses change. In essence, the alteration made by the Brans-Dicke theory manifests itself as a scalar field source. However, the physical

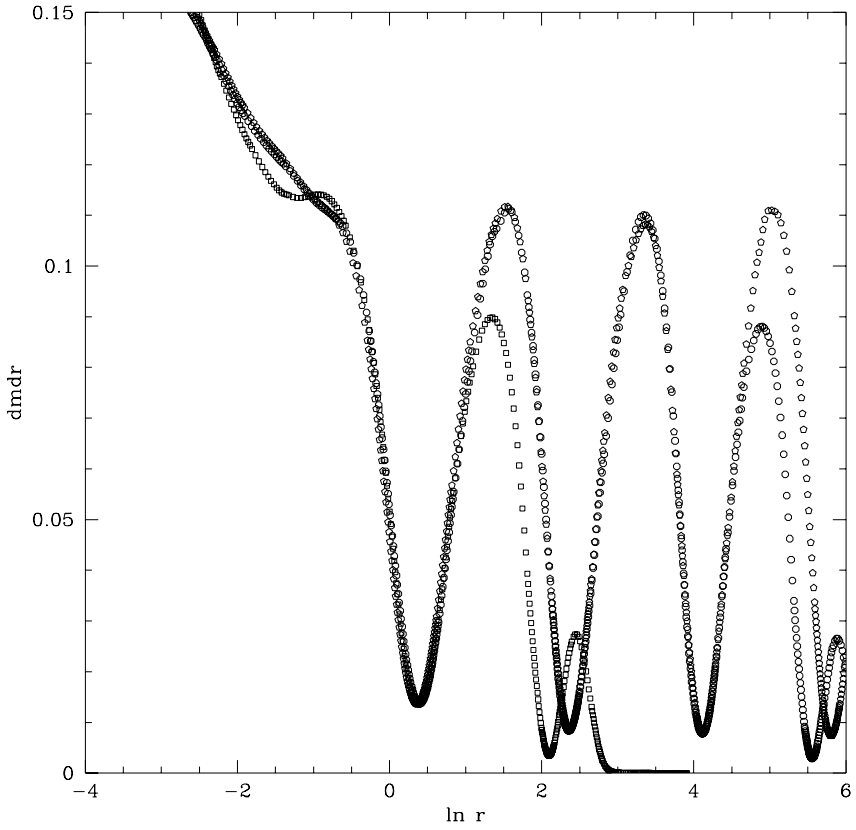

Figure 3.5: Evidence for scale periodicity

effects of the Brans-Dicke effects are evident only in the Brans-Dicke frame.

To observe the actual physical parameters of the system, I make the transformation back to the Brans-Dicke frame via

$$g_{ab} = \frac{1}{\phi}\bar{g}_{ab} \tag{3.10}$$

Thus, the metric functions a and α, for which the model has solved, now become

$$\bar{g}_{tt} = \alpha^2 \rightarrow \frac{1}{\phi}\alpha^2 \tag{3.11}$$

$$\bar{g}_{rr} = a^2 \rightarrow \frac{1}{\phi}a^2 \tag{3.12}$$

The most tangible of the parameters studied here is certainly the mass aspect function $m(r,t)$. However, the relation by which this function is found was obtained by associating metric components with the Schwarzschild metric. In the Brans-Dicke frame, the field equations are not those of general relativity, and the Schwarzschild solution is not guaranteed to hold. Thus, the mass is a much more complicated matter than in the Einstein frame.

According to [Lee,1974], the scalar mass associated with the Brans-Dicke field can be expressed concisely by

$$M_s(t) = \frac{r}{2}\left(\phi - 1\right) \tag{3.13}$$

when calculating in an asymptotically flat, static region. These conditions are satisfied only at both the beginning of the simulation and the end, after the scalar field has radiated out of the computational domain.

In [Scheel,1995b], the authors find the scalar mass as function for time for Oppenheimer-Snyder collapse of collisionless particles. For comparison

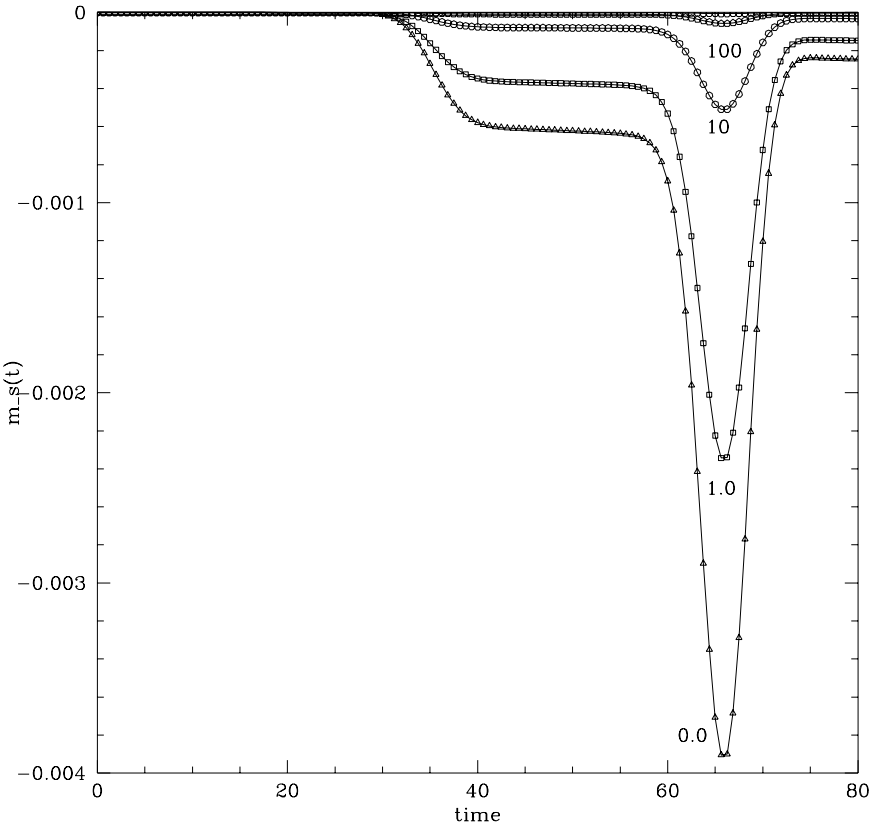

Figure 3.6: Scalar mass for the Brans-Dicke frame

purposes, figure 3.6 displays the values of the scalar mass computed from (3.13) at the outer boundary for different values of ω. The results appear consistent with features found in their graph. Beginning with some small initial scalar mass, suffering some extreme dynamics (which are not considered meaningful given that the region is far from static or flat during these times), the mass eventually settles to zero once the scalar field has radiated away.

Despite the apparent complexity involved in specifying mass in the Brans-Dicke frame, work by Hawking [Hawking,1972] has shown that a Brans-Dicke black hole will reach a static solution equivalent to a Schwarzschild black hole. With this result, I surmise that the mass scaling found in the Einstein frame is similar to that in the Brans-Dicke frame. All holes found for the mass scaling relation in the Einstein frame can be transformed back to the Brans-Dicke frame at some late time such that the fields have radiated away their energies. At these late times, the masses can be transformed back. Thus, the scaling should hold, but perhaps with a different scaling exponent.

Chapter 4

Conclusion

4.1 Results compared to those for Einstein Equations

It is interesting to consider the case when no matter field is present. With the entire model defined by the equations (2.60 - 2.63, 2.82 - 2.86), setting $\Phi = 0 = \Pi$ eliminates all matter from the equations. Only the Brans-Dicke field is present coupling to gravity. By inspection, this case is just one scalar field coupled to gravity. In other words, up to a constant, the situation is identical to that in which Choptuik finds the interesting critical phenomena[Choptuik,1993]. Because the situation is identical, indeed the results for the universal exponents should equal those which Choptuik found.

The results found in the previous chapter did confirm those in Choptuik's work[Choptuik,1993]. I did find, by varying a parameter p of the initial pulse, that the Brans-Dicke field formed black holes with mass M_{BH} according to

$$M_{BH} = c_i|p - p^*|^\gamma \tag{4.1}$$

where p^* was the critical value of p which separates the two regimes in which black holes did and did not form. Both Choptuik and I found for the mass scaling exponent $\gamma = 0.37$.

The results also demonstrated the scale periodic behavior of the near critical evolution in the area near the center. For the spatial scaling exponent,

I found $\Delta_\rho \approx 3.37$ while Choptuik found $\Delta_\rho \approx 3.44$. The discrepancy is apparently due to the method of fitting. Choptuik computes Δ_ρ by fitting the profiles at the times during which they are evolving. I arrived at my value by fitting the profiles at some late time by which time the features have had a chance to propagate outwards. Choptuik's fit is both more sophisticated and more accurate.

In a similar manner, one can attempt to remove the Brans-Dicke field by setting $\phi(r, t = 0) = 1$ for all r so that $P = 0 = Q$ initially. However, equation (2.61) shows that the time derivative of P is not necessarily zero for $P(r, t = 0) = 0 = Q(r, t = 0)$. Indeed, the second term of the right side of equation (2.61) is expressed only in terms of Φ and Π, the derivatives of the matter field. Thus, setting the Brans-Dicke field to a constant, only serves to remove the effect of the Brans-Dicke field at the initial time. The coupling of the Brans-Dicke field to the matter field results in development of features in the initially quiescent Brans-Dicke field.

4.2 For Future Study ...

Clearly, interpreting the results in the context of the Brans-Dicke frame has not been completed. Assigning a dynamical mass to the Brans-Dicke field appears quite difficult. Lee [Lee,1974] derives various conserved mass quantities in the context of superpotentials. Calculations based on the approach of [Lee,1974] appears to hold the best hope for interpreting the results in the Brand-Dicke frame.

Another avenue under investigation is the search for a universal be-

havior for multiple scalar fields in the same universe. Choptuik [Choptuik,1995] has found evidence that multiple independent scalar fields in general relativity produce critical solutions identical to the single field case up to some scaling factor. He proposes that the situation studied in this thesis, which amounts to two scalar fields coupled to Einstein gravity, might also transform such that the two transformed fields produce identical critical solutions. Specifically, if X_1^*, Y_1^* represent the critical profiles of one field, and X_2^*, Y_2^* represent those of the other, then it may be possible to find two transformed fields such that

$$\frac{dm^*}{dr} = \sigma_1 \left(X_1^{*2} + Y_1^{*2} \right) + \sigma_2 \left(X_2^{*2} + Y_2^{*2} \right) \tag{4.2}$$

For the case in which this result held, he had

$$\Box \phi_i = 0 \tag{4.3}$$

for all fields ϕ_i. With the fields studied here in the Einstein frame, their wave equations appear

$$\begin{aligned} \Box \xi &= -4\pi \lambda e^{-\xi} g^{\mu\nu} \psi_{,\mu} \psi_{,\nu} \\ \Box \psi &= g^{\mu\nu} \psi_{,\mu} \xi_{,\nu} \end{aligned} \tag{4.4}$$

I have not yet found a transformation which takes these terms to zero or at least the same potential. Further work is needed.

The results presented here have shown conclusively that the mass scaling and scale-periodic critical effects are present in the Brans-Dicke theory. Further study of the mixed case containing both the matter field ψ and the Brans-Dicke field ϕ is necessary. Preliminary findings clearly indicate the same effects appear, however, measurements have yet to be taken.

BIBLIOGRAPHY

[ADM,1962] Arnowitt, R., S. Deser and C. W. Misner. "The Dynamics of General Relativity." in *Gravitation-An Introduction to Current Research*, L. Witten, ed. New York: Wiley, 1962.

[Bechmann,1995] Bechmann, O. and O. Lechtenfeld. "Exact Black-Hole Solution With Self-Interacting Scalar Field." LANL[1] Preprint, gr-qc/9502011 (1995).

[Berger,1984] Berger, M. J. and J. Oliger. "Adaptive Mesh Refinement for Hyperbolic Partial Differential Equations." *J. Comp. Phys.* **53** (1984), pgs. 484-512.

[Brans,1961] Brans, C. and R. H. Dicke. "Mach's Principle and a Relativistic Theory of Gravitation." *Phys. Rev.* **124**, 1961 pgs. 925-35.

[Choptuik,1986] Choptuik, Matthew. Ph. D. Dissertation. Department of Physics, U. B. C., Vancouver, British Columbia. July 1986.

[Choptuik,1995] Choptuik, Matthew. Notes and conversation, 1995.

[Choptuik,1994] Choptuik, Matthew. `ad` *: An Implementation of the Berger-Oliger Mesh Refinement Algorithm For the Wave Equation in Spherical*

[1]Citations to LANL Preprint xxx/999999 are references to preprints deposited in the electronic archives maintained at Los Alamos National Laboratory.

Symmetry. University of Texas at Austin, Center for Relativity, Technical Report UTREL/TR94-001.

[Choptuik,1993] Choptuik, Matthew. "Universality and Scaling in Gravitational Collapse of a Massless Scalar Field," *Physical Review Letters*. **70**,1 (Jan, 1993) pgs. 9-12.

[Choptuik,1991] Choptuik, Matthew. "Consistency of Finite-Difference Solutions of Einstein's Equations," *Physical Review D*. **44**,10. Nov. 1991, pgs. 3124-3135.

[Garfinkle,1995] Garfinkle, David. *Choptuik Scaling in Null Coordinates*. LANL Preprint, gr-qc/9412008 (1994).

[Hawking,1972] Hawking, S. W. "Black Holes in the Brans-Dicke Theory of Gravitation." *Comm. Math. Phys.* **25**, 1972. pgs 167-71.

[Koike,1995] Koike, Tatsuhiko, T. Hara, and S. Adachi. *Critical Behavior in Gravitational Collapse of Radiation Fluid*. LANL Preprint, gr-qc/9503007 (1995).

[Lee,1974] Lee, D. L. "Conservation Laws, Gravitational Waves, and Mass Losses in the Dicke-Brans-Jordan Theory of Gravity." *Phys. Rev. D.* **10**, 1974, pgs. 2374-83.

[Misner,1973] Misner, C. W., K. S. Thorne, and J. A. Wheeler. *Gravitation*. New York: Freeman, 1973. Chapter 21.

[Richardson,1910] Richardson, L. F. "The Approximate Arithmetical Solution by Finite Differences of Physical Problems Involving Differential Equations, with an Application to the Stresses in a Masonry Dam." *Phil. Trans. Roy. Soc.* **210**, 1910, pgs. 307-57.

[Scheel,1995a] Scheel, M. A., S. L. Shapiro, and S. A. Teukolsky,. "Collapse to Black Holes in Brans-Dicke Theory, Part I". Submitted to *Phys. Rev. D* LANL Preprint, gr-qc/9411025 (1994).

[Scheel,1995b] Scheel, M. A., S. L. Shapiro, and S. A. Teukolsky,. "Collapse to Black Holes in Brans-Dicke Theory, Part II". Submitted to*Phys. Rev. D* LANL Preprint, gr-qc/9411026 (1994).

[Wald,1984] Wald, R. M. *General Relativity.* Chicago: Univ. of Chicago, 1984, pgs. 445-9.

[Weinberg,1972] Weinberg, Steven. *Gravitation and Cosmology.* New York: Wiley, 1972, pgs. 157-160.

[York,1979] York, J. W. "Kinematics and Dynamics of General Relativity." *Sources of Gravitational Radiation.* Cambridge: Cambridge University Press, 1979. pgs. 83-126.

VITA

Steven Lawrence Liebling was born in Phoenix, Arizona on November 27, 1970, the son of Carol Sue Liebling and Norman Harris Liebling. After completing his work at Clear Lake High School in Houston, Texas in 1989, he traveled north to study physics at Brown University. He spent his junior year abroad studying Chinese at the Chinese University of Hong Kong. He received an A.B. from Brown University in May, 1993. After completing further research under Peter Timbie, Physics Professor at Brown University, he entered The Graduate School at The University of Texas in August, 1993.

Permanent address: 15006 Pleasant Valley
Houston, Texas 77062

This thesis was typed by the author.